THE JOURNAL OF BIOLOGICAL CHEMISTRY VOL. 291, NO. 45, pp. 23390–23402, November 4, 2016

Adrenomedullin 2 Enhances Beiging in White Adipose Tissue Directly in an Adipocyte-autonomous Manner and Indirectly through Activation of M2 Macrophages*[S]

Received for publication, April 30, 2016, and in revised form, August 28, 2016 Published, JBC Papers in Press, September 12, 2016, DOI 10.1074/jbc.M116.735563

Ying Lv[‡], Song-Yang Zhang[‡], Xianyi Liang[‡], Heng Zhang[§], Zhi Xu[¶], Bo Liu[‡], Ming-Jiang Xu[‡], Changtao Jiang[‡1], Jin Shang[‖2], and Xian Wang[‡]

From the [‡]Department of Physiology and Pathophysiology, School of Basic Medical Sciences, Peking University, Key Laboratory of Molecular Cardiovascular Science, Ministry of Education, and Beijing Key Laboratory of Cardiovascular Receptors Research, Beijing 100191, China, the [§]Department of Endocrinology, Beijing Chao-Yang Hospital, Capital Medical University, Beijing 100020, China, the [¶]Department of General Surgery, Peking University Third Hospital, Beijing 100191, China, and the [‖]Department of Cardiometabolic Disease, Merck Research Laboratories, Merck & Co, Inc., Kenilworth, New Jersey 07033

Adrenomedullin 2 (ADM2) is an endogenous bioactive peptide belonging to the calcitonin gene-related peptide family. Our previous studies showed that overexpression of ADM2 in mice reduced obesity and insulin resistance by increasing thermogenesis in brown adipose tissue. However, the effects of ADM2 in another type of thermogenic adipocyte, beige adipocytes, remain to be understood. The plasma ADM2 levels were inversely correlated with obesity in humans, and adipo-ADM2-transgenic (tg) mice displayed resistance to high-fat diet-induced obesity with increased energy expenditure. Beiging of subcutaneous white adipose tissues (WAT) was more noticeably induced in high-fat diet-fed transgenic mice with adipocyte-ADM2 overexpression (adipo-ADM2-tg mice) than in WT animals. ADM2 treatment in primary rat subcutaneous adipocytes induced beiging with up-regulation of UCP1 and beiging-related marker genes and increased mitochondrial uncoupling respiration, which was mainly mediated by activation of the calcitonin receptor-like receptor (CRLR)·receptor activity-modifying protein 1 (RAMP1) complex and PKA and p38 MAPK signaling pathways. Importantly, this adipocyte-autonomous beiging effect by ADM2 was translatable to human primary adipocytes. In addition, M2 macrophage activation also contributed to the beiging effects of ADM2 through catecholamine secretion. Therefore, our study reveals that ADM2 enhances subcutaneous WAT beiging via a direct effect by activating the CRLR·RAMP1-cAMP/PKA and p38 MAPK pathways in white adipocytes and via an indirect effect by stimulating alternative M2 polarization in macrophages. Through both mechanisms, beiging of WAT by ADM2 results in increased energy expenditure and reduced obesity, suggesting ADM2 as a novel anti-obesity target.

An imbalance between energy intake and energy expenditure is the cause for the development of obesity, which is a high risk factor for type 2 diabetes and related metabolic disorders. Adaptive thermogenesis in adipose tissue is an important contributor to overall energy expenditure; thus, enhancing thermogenesis in adipose tissue is considered one of the promising therapeutic strategies to improve energy homeostasis (1).

In contrast to white adipose tissue (WAT),[3] which stores energy as triglycerides, brown adipose tissue (BAT) dissipates energy as heat by uncoupling protein 1 (UCP1)-mediated uncoupling of the mitochondrial respiratory chain from ATP synthesis (2). Upon stimuli such as β-3 adrenergic agonists or cold challenge, some adipocytes within WAT can exhibit brown-like features (3, 4) and have been identified as the third type of adipocytes, named "brite" (brown-in-white) or "beige" adipocytes (5). This biological process is referred to as WAT "browning" or "beiging" (3).

Studies in both rodents and humans indicated that beiging of WAT increases the whole-body metabolic rate and improves energy homeostasis in obesity and type 2 diabetes (3, 6–10). Enhancing WAT beiging alone was sufficient to alleviate obesity in mice (6), and emerging evidence also suggests that human thermogenic adipocytes are more similar to mouse beige adipocytes than to mouse brown adipocytes (11, 12). Therefore, promoting WAT beiging has attracted great interest as a potential therapeutic approach for metabolic disorders.

Several endogenous secretory factors can directly activate beiging of white adipocytes in a cell-autonomous fashion,

* This work was supported by National Natural Science Foundation of the People's Republic of China Grants 31230035 and 91439206 (to X. W.) and 81522007 and 81470554 (to C. J.), National Basic Research Program (973 Program) of the People's Republic of China Grant 2012CB518002 (to M. J. X.), 111 Project of the Chinese Ministry of Education Grant B07001, and a Merck Sharp & Dohme R&D China postdoctoral fellowship (to Y. L.). J. S. is an employee of Merck & Co., Inc.

[S] This article contains supplemental Figs. S1–S3 and Tables S1 and S2.

[1] To whom correspondence may be addressed: Dept. of Physiology and Pathophysiology, School of Basic Medical Sciences, Peking University, Beijing 100191, China. Tel.: 86-10-82805613; E-mail: jiangchangtao@bjmu.edu.cn.

[2] To whom correspondence may be addressed: Dept. of Cardiometabolic Disease, Merck Research Laboratories, 2015 Galloping Hill Rd., Kenilworth, NJ 07033. Tel.: 908-455-2816; E-mail: jin_shang@merck.com.

[3] The abbreviations used are: WAT, white adipose tissue; BAT, brown adipose tissue; CGRP, calcitonin gene-related peptide; HFD, high-fat diet; BMI, body mass index; scWAT, subcutaneous white adipose tissue; tg, transgenic; Fgf21, fibroblast growth factor 21; FCCP, carbonyl cyanide *p*-trifluoromethoxyphenylhydrazone; OCR, oxygen consumption rate; RNAseq, RNA sequencing; qPCR, quantitative RT-PCR; TMRM, tetramethylrhodaminemethyl ester; CRLR, calcitonin receptor-like receptor; RAMP, receptor activity-modifying protein; Th, tyrosine hydroxylase; Ddc, dopa decarboxylase; Dbh, dopamine β-hydroxylase; NE, norepinephrine; SVC, primary stromal vascular cell; PE, phosphatidylethanolamine; PKI, protein kinase inhibitor; APC, allophycocyanin; ANOVA, analysis of variance.

including adrenergic hormones such as catecholamines (13), Fgf 21, irisin, methionine-enkephalin peptide, cardiac natriuretic peptide, and bone morphogenetic proteins (8, 14–18). Additionally, recent studies reported that the innate immune cells within WAT, especially anti-inflammatory M2 macrophages, play crucial roles in promoting the development of beige fat (13, 19, 20). Adipocyte-secreted adiponectin, eosinophil-secreted IL-4, and group 2 innate lymphoid cell-secreted IL-13 have been shown to promote beiging via activating M2 polarization of macrophages in white adipose tissue (8, 13, 19).

Adrenomedullin 2 (ADM2), also known as intermedin, is an endogenous peptide discovered in 2004 and belongs to the calcitonin gene-related peptide (CGRP)/calcitonin family (21, 22). The homology of its mature peptide between rodents and humans is rather high (mouse *versus* rat, 97.9%; mouse *versus* human, 89.4%; human *versus* rat, 87.2%). ADM2 is ubiquitously expressed in various tissues, including adipose tissue (23, 24), and has been reported to play protective roles in the cardiovascular and renal systems via multiple mechanisms, such as anti-inflammation, inhibition of oxidative stress, and endoplasmic reticulum stress (25–28). ADM2 can be synthesized and secreted from adipocytes, and its expression is down-regulated in adipose tissues of db/db mice and high-fat diet (HFD)-induced obese mice (29). Subcutaneous ADM2 dosing by minipump implantation could improve hyperhomocysteinemia or HFD-induced insulin resistance in mice (29, 30). ADM2 was also reported to substantially inhibit adipocyte MHC II expression and thus ameliorate insulin resistance in adipose tissue (31). Previous studies from our group also demonstrated that ADM2 reduced obesity in mice associated with increased thermogenesis in BAT (29); however, the effects of ADM2 in the energy metabolism of beige fat remain largely unknown.

In this study, we investigated the roles of ADM2 in energy homeostasis and WAT beiging and explored the underlying mechanisms. Our results suggest that ADM2 is a novel endogenous beiging activator with the potential to become a new therapeutic target for obesity and related metabolic disorders.

Results

Plasma ADM2 Levels Are Inversely Correlated with Obesity in Humans—To evaluate endogenous ADM2 levels in humans with different metabolic status, plasma ADM2 levels were measured in 74 Chinese individuals. Body weight and body mass index (BMI) were observed to be inversely correlated with ADM2 plasma levels with statistical significance ($p = 0.0014$ for body weight and $p = 0.0176$ for BMI) (Fig. 1, *A* and *B*). Based on the diagnostic criteria for obesity in the Chinese population (32), the plasma ADM2 levels were lower by 32% in obese subjects (BMI $>$ 28) than in subjects with normal weight (BMI $\leq$ 24) (Fig. 1*C*), implying a strong association of ADM2 with obesity. Neither age nor gender showed a noteworthy correlation with plasma ADM2 levels (Fig. 1, *D* and *E*).

Adipocyte-ADM2 Overexpression Improves Mitochondrial Respiration and Thermogenesis in scWAT—Our previous studies have shown that ADM2 expression in adipose tissues is decreased after HFD treatment (29). Here we also observed a significant inverse relationship between the relative *Adm2* mRNA levels in WAT and animal body weight in C57BL/6J male mice ($p < 0.01$) (Fig. 2*A*). Transgenic mice overexpressing the human *ADM2* gene specifically in adipocytes (adipo-ADM2-tg mice) have been generated to study the roles of ADM2 in metabolic homeostasis regulation (supplemental Fig. S1) (29). In the transgenic mice, ADM2 expression was only increased in adipose tissues at both the transcriptional and translational levels, with a very minimal increase in macrophages at the mRNA but not at the protein level and no increase in other tissues examined (supplemental Fig. S1, *B–D*). These mice displayed less body weight and fat mass gain during 12-week HFD feeding compared with WT littermates (supplemental Fig. S2, *A* and *B*), which was in consistent with our previous observation on an 8-week HFD study (29). Adipo-ADM2-tg mice also displayed increased whole-body energy expenditure without significant differences in either food intake or ambulatory activity (supplemental Fig. S2, *C–H*), which was previously mainly attributed to the activation of thermogenesis in BAT (29). Here we further explored whether heat production from beige adipocytes additionally contributed to this elevation in systematic energy expenditure. Because scWAT is highly prone to beiging induction (5, 6), mitochondrial metabolic respiration in subcutaneous adipose depots was measured by Seahorse analyzer. There was an increase in the basal and FCCP-stimulated maximal respiration rate of oxygen consumption (OCR) in scWAT, indicating an acceleration of energy metabolism in ADM2-overexpressed adipose tissue (Fig. 2, *B* and *C*). The comparable ATP production OCR and declined coupling efficiency (Fig. 2, *C* and *D*) showed that the increased energy metabolized in the respiratory chain was not used for ATP synthesis but mostly dissipated for heat production. Consistent with this, the mRNA levels of the key thermogenesis gene *Ucp1* and mitochondrial respiration genes *Ndufb8*, *Uqcrc2*, and *Cox8b* were up-regulated in the scWAT of adipo-ADM2-tg mice (Fig. 2*E*). Moreover, the beige-selective markers *Tmem26*, *Cd137*, and *Tbx15* were also markedly up-regulated, whereas the white adipocyte-related markers *Igfbp3* and *Lep* were markedly down-regulated by adipocyte-ADM2 overexpression (Fig. 2, *F* and *G*). To rule out possible effects from other cell types in crude adipose tissues, adipocytes were specifically isolated from scWAT, and the subsequent flow cytometry analysis showed a striking increase in the beiging marker CD137 in adipocytes from adipo-ADM2-tg mice (Fig. 2*H*). Collectively, these results suggested that adipocyte-ADM2 overexpression activated beiging in scWAT with the enhancement of metabolic respiration and UCP1-mediated thermogenesis, which might make a substantial contribution to increased whole-body energy expenditure and decreased body weight in adipo-ADM2-tg mice.

Cold-induced Beiging Was Markedly Activated in scWAT of Adipo-ADM2-tg Mice—Beige adipocytes can be activated by cold exposure (7, 13). We next examined whether cold-induced beiging could be further promoted by adipocyte-ADM2 overexpression. After 48-h cold challenge at 4 °C, the subcutaneous adipocytes of adipo-ADM2-tg diet-induced obese mice showed a much greater decrease in cell size than those of WT mice (Fig. 3, *A* and *B*). The protein levels of both UCP1 and the beige marker TMEM26 in scWAT were substantially increased by

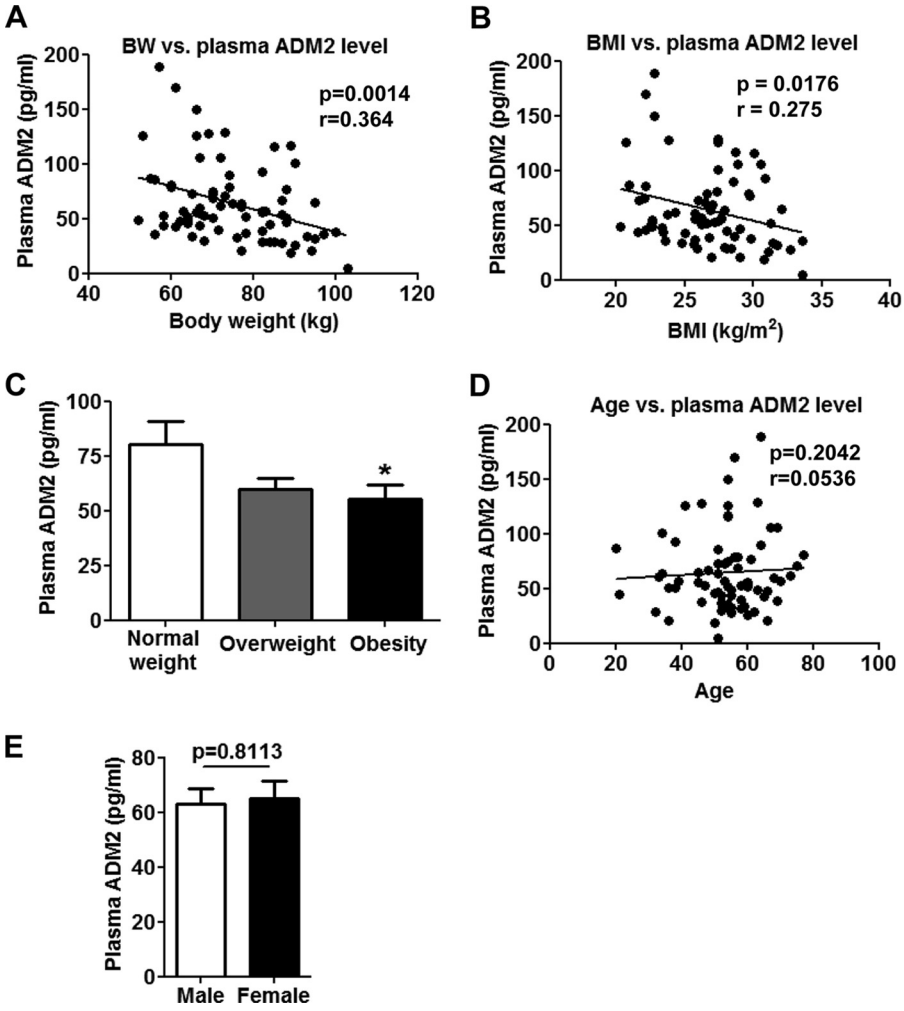

FIGURE 1. **Plasma ADM2 levels are inversely correlated with obesity in humans.** Plasma samples were collected from a total of 74 Chinese adults, and the ADM2 levels were measured by radioimmunoassay. *A*, negative correlation of body weight (*BW*) *versus* plasma ADM2 levels. *B*, inverse correlation of BMI and plasma ADM2 levels. *C*, comparison of the plasma ADM2 levels in normal (BMI $\leq$ 24), overweight (24 $<$ BMI $\leq$ 28), and obese (BMI $>$ 28) human subjects. *D*, no significant correlation of age *versus* plasma ADM2 levels. *E*, similar plasma ADM2 levels in the male (n = 38) and female (n = 36) human subjects. For group comparison (*C* and *E*), the data are represented as mean $\pm$ S.E. One-way ANOVA with Newman-Keuls test (*C*) or two-tailed Student's *t* test (*E*): *, $p < 0.05$ *versus* control. For linear regression (*A*, *B*, and *D*), the slope was considered significantly non-zero when $p < 0.05$.

adipocyte-ADM2 overexpression (Fig. 3, *C* and *D*). Additionally, adipo-ADM2-tg mice maintained thermal homeostasis at a higher body temperature than WT mice challenged with cold exposure (Fig. 3*E*). Taken together, these results indicate that adipocyte-ADM2 overexpression could enhance cold-induced beiging and thermogenesis in scWAT.

ADM2 Treatment Promotes Beiging in Vitro in an Adipocyte-autonomous Manner—To investigate how ADM2 induced beiging of white adipocytes from scWAT, rat scWAT-derived SVCs were isolated and differentiated into mature adipocytes *in vitro*. After treatment with ADM2 in cell culture, rat adipocytes were subjected to RNA sequencing (RNAseq) profiling analysis. A general up-regulation of mitochondrial respiration and thermogenesis-related genes was observed in ADM2-treated adipocytes, suggesting a white-to-beige switch at the molecular level in adipocytes by ADM2 treatment (Fig. 4*A*). qPCR analysis further verified those transcriptional changes. *Ucp1* expression was robustly increased more than 10-fold by ADM2 treatment, and other mitochondrial respiration-related genes, including *Pgc1a*, *Ndufb8*, *Sdhb*, *Cox5b*, and *Cox8b*, were also markedly up-regulated (Fig. 4*B*). Additionally, beige-selective markers, including *Cd137*, *Tmem26*, *Fgf21*, and *Cited*, were all up-regulated, whereas the mRNA expression of white adipocyte markers, including *Retn* and *Igfbp3*, was decreased by ADM2 treatment (Fig. 4*C*). As a key thermogenesis protein in beige adipocytes (2), UCP1 was also up-regulated at the protein level, as shown by Western blotting and immunofluorescent staining (Fig. 4, *D* and *E*). Moreover, ADM2 treatment resulted in a marked increase in mitochondrial respiration in primary subcutaneous adipocytes, as measured by Seahorse analyzer (Fig. 4, *F* and *G*). The basal and maximal respiration OCRs of adipocytes were improved by 62% and 49%, respectively (Fig. 4*G*). More importantly, the uncoupling OCR was substantially elevated by nearly 2-fold, and the coupling efficiency declined from ~70% to 50% after ADM2 treatment (Fig. 4, *G* and *H*), suggesting enhanced mitochondrial uncoupling along with heat generation. Consistently, the mitochondrial membrane potential was decreased after ADM2 treatment, as shown by reduced TMRM fluorescence intensity (Fig. 4*I*). Altogether, these results indicate that ADM2 could promote white adi-

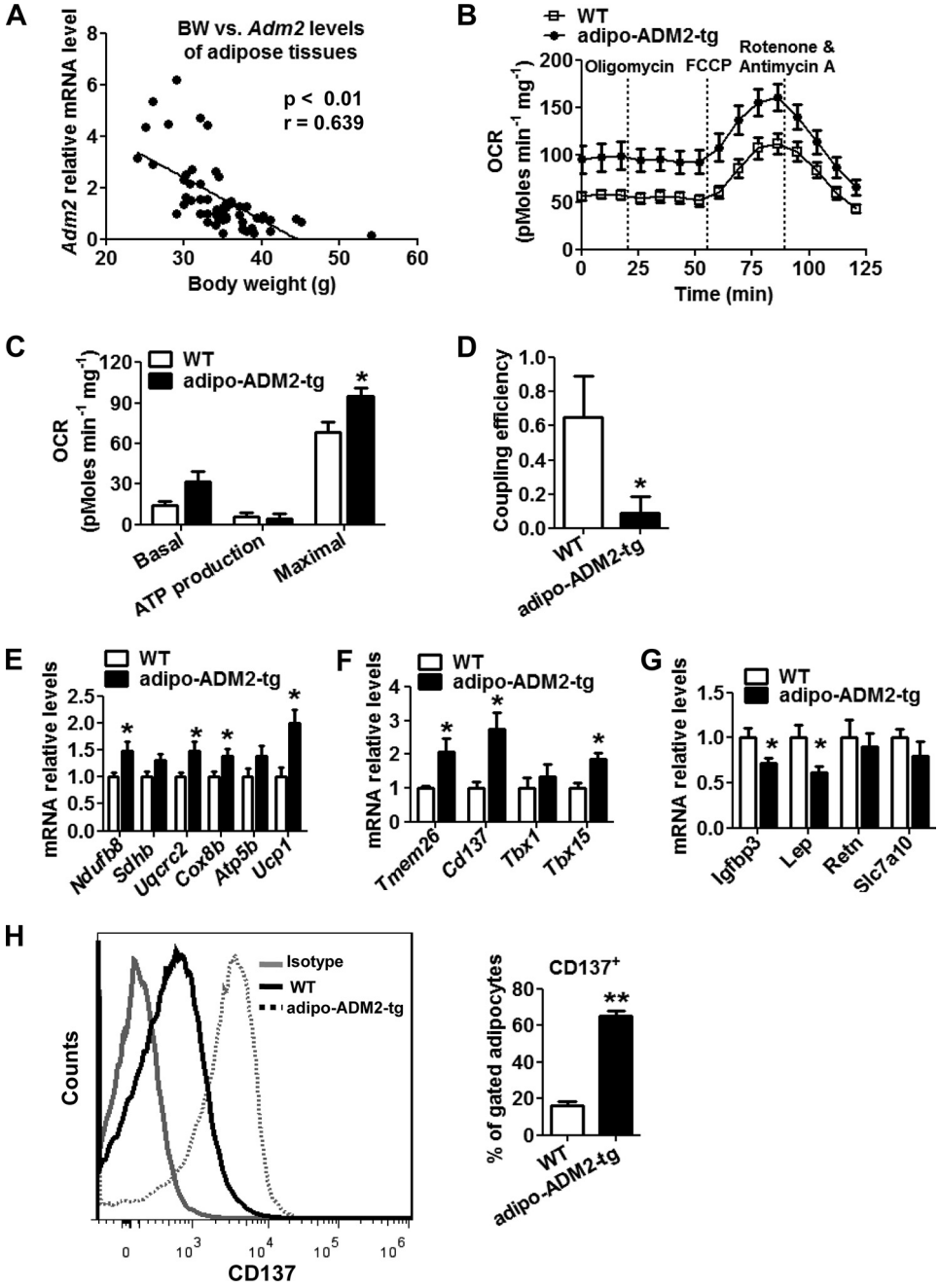

FIGURE 2. **Adipocyte-ADM2 overexpression improves mitochondrial respiration and thermogenesis in scWAT.** *A*, inverse correlation of body weight (*BW*) and relative *Adm2* mRNA levels in WAT of C57BL/6J male mice ($n = 56$). Linear regression: the slope was considered significantly non-zero when $p < 0.05$. *B–G*, Adipo-ADM2-tg mice and WT controls were fed for 12 weeks on an HFD. *B–D*, mitochondrial energetics analysis of scWAT. *B*, OCR measurement curves. *C*, basal respiration, ATP production, and maximal respiration OCR calculated from *A*. *D*, coupling efficiency (ATP production OCR/basal respiration OCR). *E–G*, relative mRNA levels of mitochondrial respiration and thermogenesis genes (*E*), beige-selective markers (*F*), and white adipocyte-selective markers (*G*) in scWAT. *H*, flow cytometry analysis of CD137 expression in mature scWAT adipocytes. The data are represented as mean ± S.E. $n = 3$ independent experiments, 4–6 mice/group. Two-tailed Student's *t* test: *, $p < 0.05$ *versus* WT; **, $p < 0.01$ *versus* WT.

pocytes beiging and increased UCP1-mediated thermogenesis in a cell-autonomous manner.

ADM2 Up-regulates UCP1 Expression in Adipocytes Mainly through the CRLR·RAMP1-cAMP/PKA and p38 MAPK Pathways—We next explored the underlying signal transduction mechanisms for the adipocyte-autonomous beiging effects by ADM2. The receptor complexes of ADM2 are composed of a calcitonin-receptor-like receptor (CRLR) and one of the three receptor activity-modifying proteins (RAMPs) (21). *Ucp1* up-regulation by ADM2 in adipocytes was markedly attenuated by the CRLR non-selective antagonist ADM17-47 (65%) and by the CRLR-RAMP1-selective antagonist CGRP8-37 (58%) but not by the CRLR-RAMP2- and CRLR-RAMP3-selective antagonist ADM22-52 (Fig. 5*A*), implying that CRLR-RAMP1 was the major receptor for the beiging effects of ADM2. G_s-mediated activation of adenylate cyclase represents the major signaling pathway coupled with the CRLR-RAMP receptors (33). The cellular cAMP content in adipocytes was increased by ~2-fold

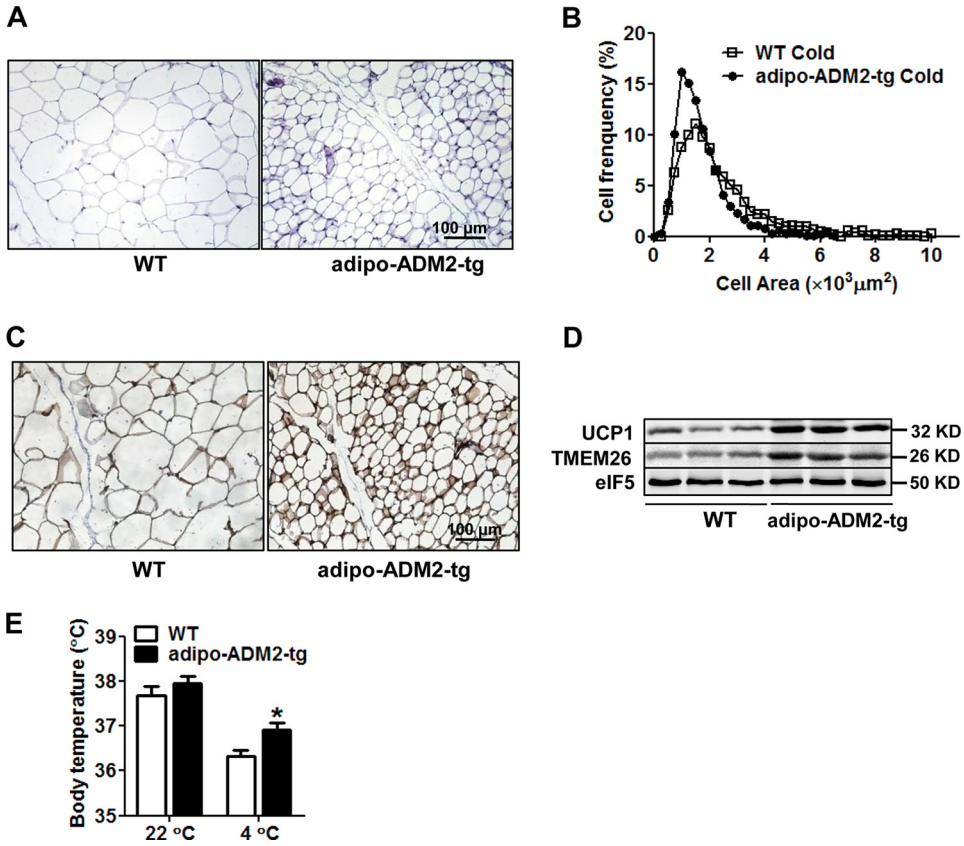

FIGURE 3. **Cold-induced beiging was markedly activated in scWAT of adipo-ADM2-tg mice.** Adipo-ADM2-tg mice and WT controls were fed an HFD for 12 weeks, followed by a 48-h cold (4 °C) exposure. *A* and *B*, H&E staining of scWAT (*A*) with adipocyte size on sections measured by ImageJ software (*B*). *C*, immunohistochemical staining of UCP1 in scWAT. *D*, immunoblotting analysis of UCP1 and TMEM26 in scWAT, with eIF5 as a loading control. *E*, body temperature. The data are represented as mean ± S.E. $n = 3$ independent experiments, 3–6 mice/group. Two-tailed Student's *t* test: *, $p < 0.05$ *versus* WT.

after ADM2 treatment (Fig. 5*B*). cAMP-dependent PKA was also activated, with PKA-mediated substrate phosphorylation increased as early as 1 h after ADM2 treatment (Fig. 5*C*). Furthermore, the cAMP antagonist Rp-cAMPS and the PKA inhibitors H89 and PKI markedly attenuated up-regulation of *Ucp1* by ADM2 by 67%, 87%, and 76%, respectively (Fig. 5*E*). The activated phosphorylation of PKA substrate by ADM2 was also suppressed by those inhibitors at the same concentration (supplemental Fig. S3*A*). The p38 MAPK pathway is considered a key pathway mediating beiging for several other endogenous peptides (14, 17, 18). Immunoblotting revealed a time-dependent elevation of phosphorylated p38 MAPK. Its phosphorylation level began to increase from 1–2 h and reached a peak 4–8 h after ADM2 treatment (Fig. 5*D*). Consistently, *Ucp1* up-regulation and p38 MAPK phosphorylation after ADM2 stimulation were both markedly attenuated by pretreatment with the p38 MAPK inhibitor SB202190 (Fig. 5*E* and supplemental Fig. S3*B*). The PI3K-Akt inhibitor LY294002 showed no inhibitory effects (Fig. 5*E*). Neither inhibitor suppressed *Ucp1* expression in adipocytes in the absence of ADM2 (supplemental Fig. S3*C*). Therefore, the direct effects of ADM2 on UCP1 up-regulation and beiging in white adipocytes were mainly mediated by the CRLR·RAMP1-cAMP/PKA and p38 MAPK pathways.

ADM2 Treatment Activates Beiging of Primary Human White Adipocytes—To address whether ADM2 was also capable of beiging activation in humans, primary human subcutaneous white adipocytes were subjected to ADM2 treatment. Consistent with the findings in rodent cells, ADM2 substantially induced the transcription of *UCP1* and the beiging-related genes *CD137* and *MTUS1* (Fig. 6*A*) and down-regulated the mRNA levels of the white adipocyte-related markers *LEP* and *IGFBP3* (Fig. 6*B*) in human primary adipocytes. UCP1 was also markedly elevated at the protein level by ADM2 treatment, as determined by both immunofluorescent staining and Western blotting (Fig. 6, *C* and *D*). Furthermore, ADM2 treatment improved the mitochondrial respiration capacity, as demonstrated by a 42% increase in maximal respiration OCR (Fig. 6, *E* and *F*). These results indicate that the adipocyte-autonomous action underlying the effect of ADM2 on WAT beiging is translatable to humans.

M2 Macrophage Activation Also Contributes to the Beiging Effects of ADM2—The anti-inflammatory M2 macrophages resident in WAT are considered an important mediator for beige adipocyte recruitment according to the latest studies (13, 19, 20). ADM2 has been reported to be anti-inflammatory and atherosclerosis-protective by regulating macrophage functions in the cardiovascular system (34, 35), which prompted us to ask whether ADM2 could induce beiging of white adipocytes in adipose tissues by cross-talk with M2 macrophages. qPCR results showed that the mRNA levels of M2 macrophage markers, including *Cd206* and *Arginase 1* (*Arg1*), were markedly up-regulated in scWAT in adipo-ADM2-tg mice, whereas the expression of M1 macrophage markers (*Cd11c* and *iNOS*) was not changed (Fig. 7*A*). Flow

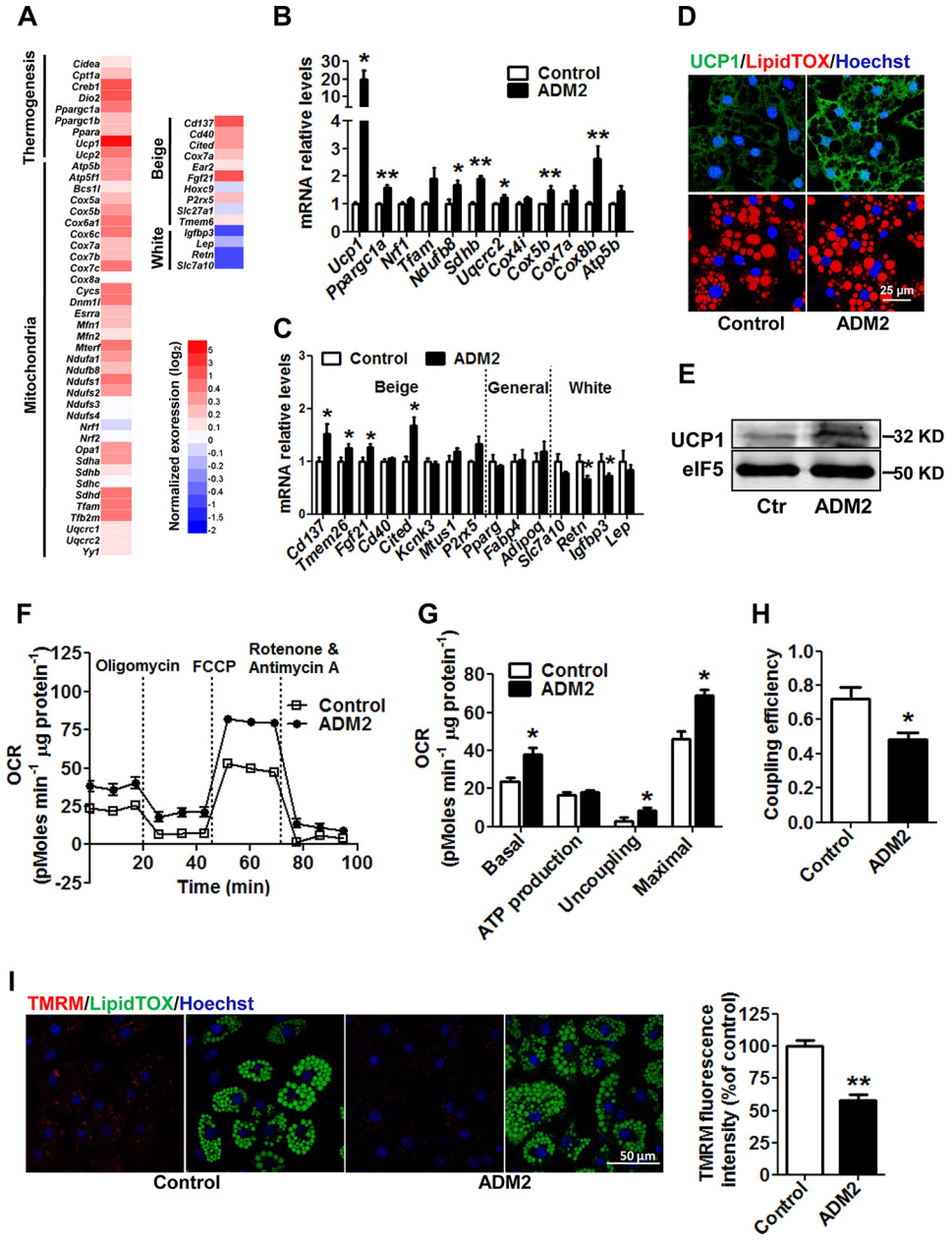

FIGURE 4. **ADM2 treatment promotes beiging *in vitro* in an adipocyte-autonomous manner.** Rat scWAT SVCs were differentiated into adipocytes and treated with 20 nM ADM2 for 8 h. *A*, heat map of the expression profiles of genes involved in mitochondrial respiration, thermogenesis, and adipocyte phenotype identity by RNAseq analysis. *B* and *C*, relative mRNA levels of mitochondrial respiration and thermogenesis genes (*B*) and beige and white adipocyte markers (*C*) by qPCR analysis. *D*, immunofluorescence staining of UCP1 (*green*) with nuclei stained by Hoechst33258 (*blue*) and lipid droplets stained by LipidTOX (*red*). *E*, immunoblotting analysis of UCP1 with eIF5 used as a loading control (*Ctr*). *F–H*, mitochondrial energetics analysis. *F*, OCR measurement curves. *G*, basal respiration, ATP production, uncoupling, and maximal respiration OCR calculated from *F*. *H*, coupling efficiency (ATP production OCR/basal respiration OCR). *I*, TMRM staining (*red*) of adipocytes, with nuclei stained by Hoechst 33258 (*blue*) and lipid droplets stained by LipidTOX (*green*). TMRM fluorescence intensity was quantified by ImageJ software and normalized by nucleus number. The data are represented as mean ± S.E. $n = 3$ independent experiments (3–6 samples/experiment). Two-tailed Student's *t* test: *, $p < 0.05$ *versus* control; **, $p < 0.01$ *versus* control.

cytometry analysis consistently demonstrated a marked increase in the percentage of M2 macrophages (F4/80+, CD206+, CD11c−) within the stromal vascular fraction of scWAT in adipo-ADM2-tg mice compared with WT animals (Fig. 7*B*), displaying an accumulation of M2 macrophages in scWAT by ADM2 overexpression. Mouse peritoneal macrophages were isolated and treated with ADM2 *in vitro*. Up-regulation of the M2 marker Arg1 in macrophages at both the mRNA and protein levels after 12-h ADM2 treatment showed that ADM2 could directly induce M2 polarization in macrophages (Fig. 7, *C* and *D*). Local catecholamine secretion from M2 macrophages in WAT is a crucial inducer for beige fat recruitment through the direct stimulation of β3 adrenergic receptor on adipocytes (13, 20). Tyrosine hydroxylase (Th), dopa decarboxylase (Ddc), and dopamine β-hydroxylase (Dbh) are three key enzymes for catecholamine synthesis, and ADM2 treatment resulted in a substantial increase in the protein levels of Th and a small but significant increase in Ddc in macrophages (Fig. 7*E*). Furthermore, norepinephrine (NE) secretion for 8 h from

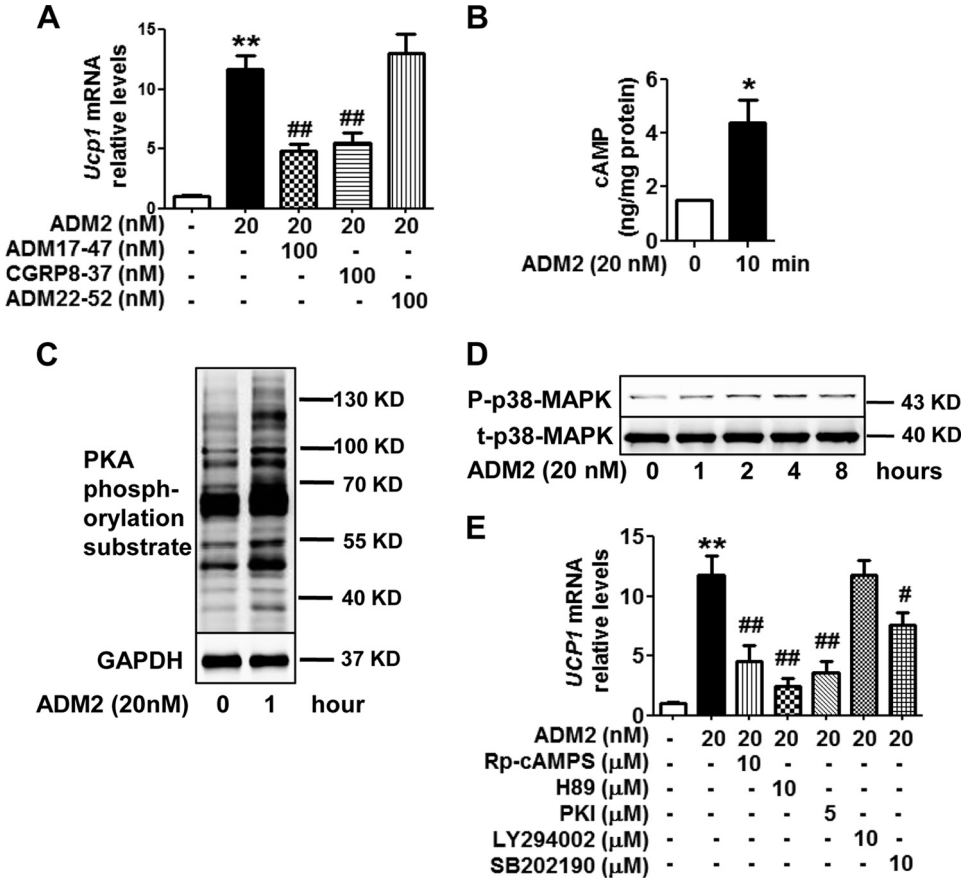

FIGURE 5. **ADM2 up-regulates UCP1 expression in adipocyte mainly through the CRLR·RAMP1-cAMP/PKA and p38 MAPK pathways.** Rat scWAT SVCs were differentiated into adipocytes and treated with ADM2. *A* and *E*, Relative mRNA levels of *Ucp1* in adipocytes treated with ADM2 for 8 h with or without 1-h pretreatment of CRLR-RAMP receptor antagonists (*A*) or signaling pathway inhibitors (*E*). *B*, cellular cAMP levels. *C* and *D*, immunoblotting analysis of phosphorylation levels of PKA-mediated substrates (*C*) and p38 MAP kinase (*D*) in adipocytes. The data are represented as the mean ± S.E. $n = 3$ independent experiments (3–6 samples/experiment). One-way ANOVA with Newman-Keuls test (*A* and *E*) or two-tailed Student's *t* test (*B*): *, $p < 0.05$ *versus* control; **, $p < 0.01$ *versus* control; #, $p < 0.05$ *versus* ADM2 treatment; ##, $p < 0.01$ *versus* ADM2 treatment.

ADM2-treated macrophages was more than 2-fold that from control cells (Fig. 7*F*).

To determine whether the catecholamine released by ADM2-treated macrophages was sufficient to enhance beiging of adipocytes, conditional medium collected from macrophages was transferred to incubate adipocytes (Fig. 8*A*). *Ucp1* expression in adipocytes was markedly elevated by ~2-fold with the conditional medium from ADM2-treated macrophages compared with that from control macrophages. Moreover, this increase in *Ucp1* expression could be blocked by propranolol, a β-adrenergic receptor antagonist (Fig. 8*B*). Taken together, these results suggested that M2 polarization along with increased catecholamine secretion from macrophages is an additional important mechanism underlying the beiging effects of ADM2 scWAT.

Discussion

Our previous researches regarding the metabolic benefits of ADM2 mainly focused on the activation of BAT (29). In this study, we further demonstrated the beneficial effects of ADM2 on energy homeostasis and highlighted its roles in enhancing WAT beiging. The results of our study collectively point to a working model for the effects of ADM2 on WAT beiging, as illustrated in Fig. 8*C*. On one hand, ADM2 interacts with the CRLR-RAMP1 receptor complex on white adipocytes and stimulates G_s-mediated activation of adenylate cyclase, resulting in the cAMP-dependent activation of PKA. p38 MAPK is also activated in response to ADM2 stimulation. These two kinases further drive the up-regulation of thermogenesis- and beiging-related genes, including UCP1, and lead to beiging of white adipocytes directly. On the other hand, ADM2 acts on resident macrophages in WAT and stimulates M2 polarization along with catecholamine secretion, which, in turn, activates the β3 adrenergic receptor on adipocytes and enhances beiging indirectly. Beige adipocytes activated by the above two mechanisms dissipate excess energy through metabolic thermogenesis, thus improving systematic energy homeostasis and alleviating obesity and related metabolic disorders.

Because scWAT is highly prone to beiging induction compared with visceral WAT (5, 6), we chiefly focused on fat pads from subcutaneous fat depots in animal models and adopted differentiated scWAT adipocytes for all *in vitro* experiments. In addition to the expressional changes in thermogenesis- and beiging-related genes, this study further demonstrated ADM2-mediated improvement of mitochondrial respiration in both *ex vivo* isolated subcutaneous fat tissues as well as *in vitro* differ-

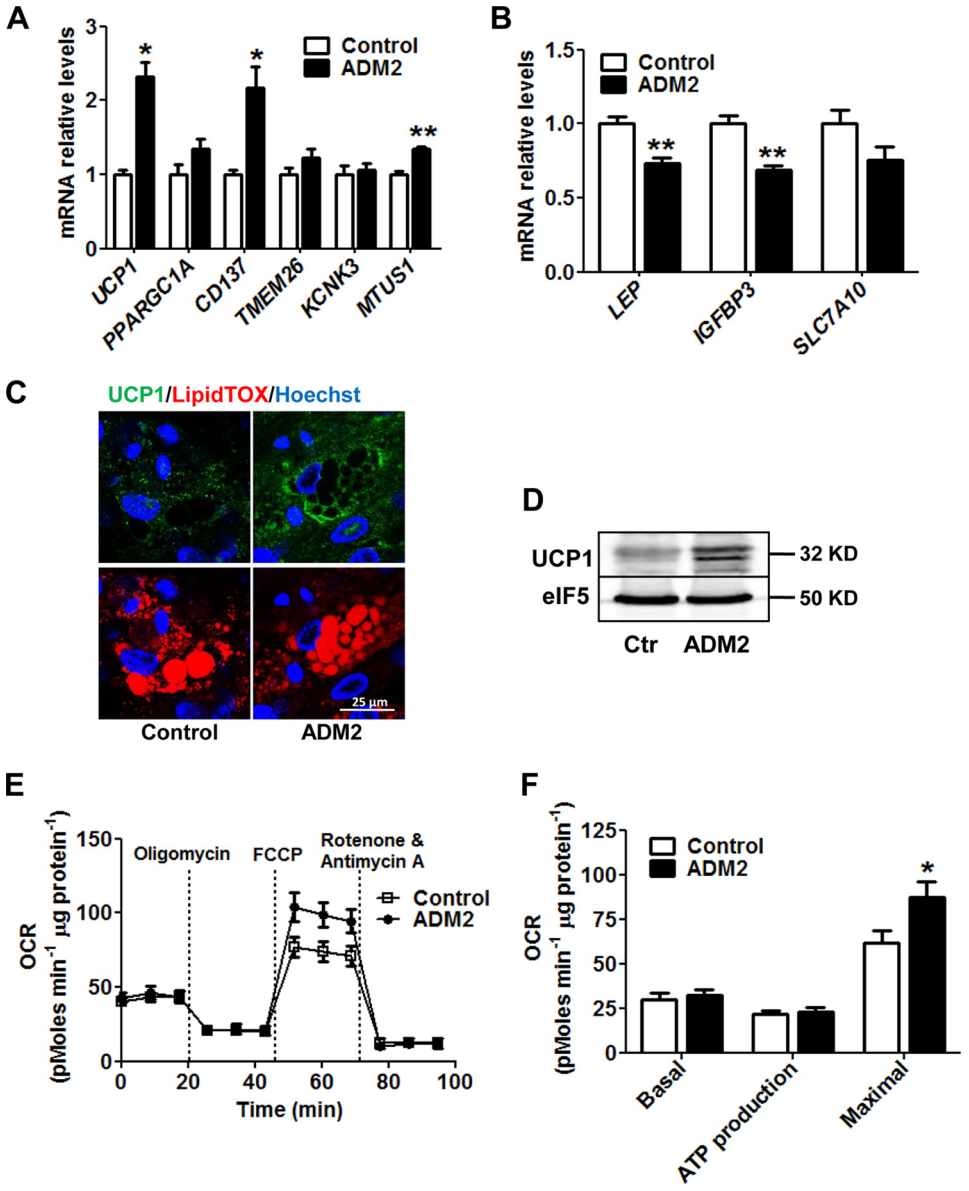

FIGURE 6. **ADM2 treatment activates beiging of primary human white adipocytes.** Primary human scWAT SVCs were differentiated into adipocytes and treated with 20 nM ADM2 for 8 h. *A* and *B*, relative mRNA levels of *UCP1* and adipocyte markers. *C*, immunofluorescence staining of UCP1 (*green*) with nuclei stained by Hoechst 33258 (*blue*) and lipid droplets stained by LipidTOX (*red*). *D*, immunoblotting analysis of UCP1 with eIF5 used as a loading control (*Ctr*). *E* and *F*, mitochondrial energetics analysis. *E*, OCR measurement curves. *F*, basal respiration, ATP production, and maximal respiration OCR calculated from *E*. The data are represented as mean ± S.E. $n = 3$ independent experiments (3–6 samples/experiment). Two-tailed Student's *t* test: *, $p < 0.05$ *versus* control; **, $p < 0.01$ *versus* control.

entiated subcutaneous adipocytes. These results provide direct functional evidence to support the beiging effects of ADM2 in scWAT.

PKA and p38 MAPK are both reported key signaling mediators for white adipocyte beiging (14, 17, 18, 36). PKA drives beiging-related transcriptional responses via the activation of cAMP-response element-binding protein and PGC-1α (7). p38 MAPK is necessary for UCP1 expression through activating ATF2 and PGC-1α (36) and is activated in response to cAMP/PKA signaling (37). In our study, phosphorylation of p38 MAPK also followed PKA induction, suggesting that p38 MAPK might be a downstream effecter of PKA in the ADM2-activated signaling pathway, but the precise relationship between these two signals needs to be further clarified. TSC1-mTORC1 signaling has recently been identified as a linker between extracellular signals and transcriptional factors to initiate the brown-to-white adipocyte phenotypic switch (38). Whether this pathway is also down-regulated upon ADM2 treatment is worth further investigation.

It has been well recognized that anti-inflammatory M2 macrophages serve as an important source of catecholamine for beiging activation in scWAT (13, 19, 20). Endogenous secretors such as IL-4, IL-13, and adiponectin have been reported to promote beiging of white adipocytes via cross-talk with resident macrophages in WAT (8, 13, 19). In this study, we also observed a marked activation of beiging accompanied by an accumulation of M2 macrophages in scWAT in adipo-ADM2-tg mice. *In vitro* studies also displayed M2 polarization of primary mouse

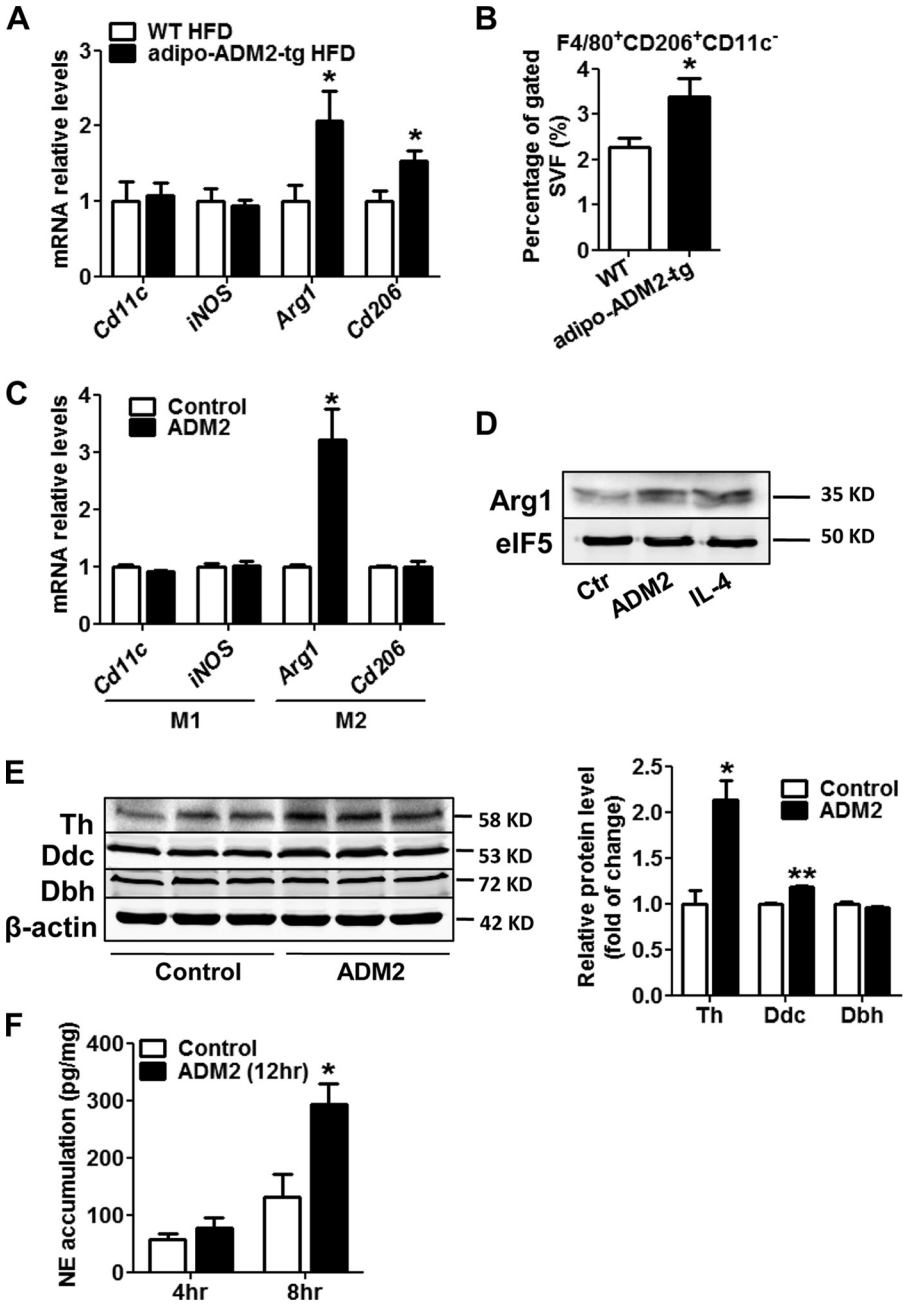

FIGURE 7. **M2 macrophage activation also contributes to the beiging effects of ADM2.** *A* and *B*, adipo-ADM2-tg mice and WT controls were fed for 12 weeks on an HFD. *A*, relative mRNA levels of M1/M2 macrophage markers in scWAT. *B*, flow cytometry analysis of M2 macrophages in the scWAT stromal vascular fraction. *C–F*, primary mouse peritoneal macrophages were treated with 20 nM ADM2 for 12 h. *C*, relative mRNA levels of M1 and M2 macrophage markers with 18S rRNA used as a normalization gene. *D*, immunoblotting analysis of Arg1, and eIF5 was used as a loading control (*Ctr*). IL4 is an M2 polarization stimulator and was used as a positive control. *E*, immunoblotting analysis of Th, Ddc, and Dbh, with β-actin as a loading control. *F*, NE accumulation in the medium of macrophages for the indicated time course. Data are represented as mean ± S.E. $n = 3$ independent experiments (3–4 mice/group, 3–6 cell samples/experiment). Two-tailed Student's *t* test: *, $p < 0.05$ *versus* control; **, $p < 0.01$ *versus* control.

macrophages after ADM2 treatment. It has been shown before that the CRLR-cAMP/PKA-pPTEN pathway is responsible for ADM2 inhibition of acetylated low-density lipoprotein uptake in macrophages (25), but the receptor and transduction signals involved in its M2 activation need to be addressed in the future. This study indicates that M2 macrophages also serve as a crucial contributor to the ADM2-mediated beiging effect in scWAT.

The cellular origin of beige adipocytes has not been completely elucidated. A bipotential precursor population capable of *de novo* beige and white differentiation has been identified (39). Beige fat biogenesis can be enhanced in multiple ways, such as stimulation of bipotential precursor proliferation, promotion of their subsequent commitment to the beige lineage (40), and induction of phenotype switch in differentiated white adipocytes (41). Our *in vitro* results collectively showed that ADM2 could exert its effects on differentiated adipocytes, thus possibly induce beiging by stimulating white-to-beige conversion. Whether other mechanisms related to beige precursors are also involved requires further investigation.

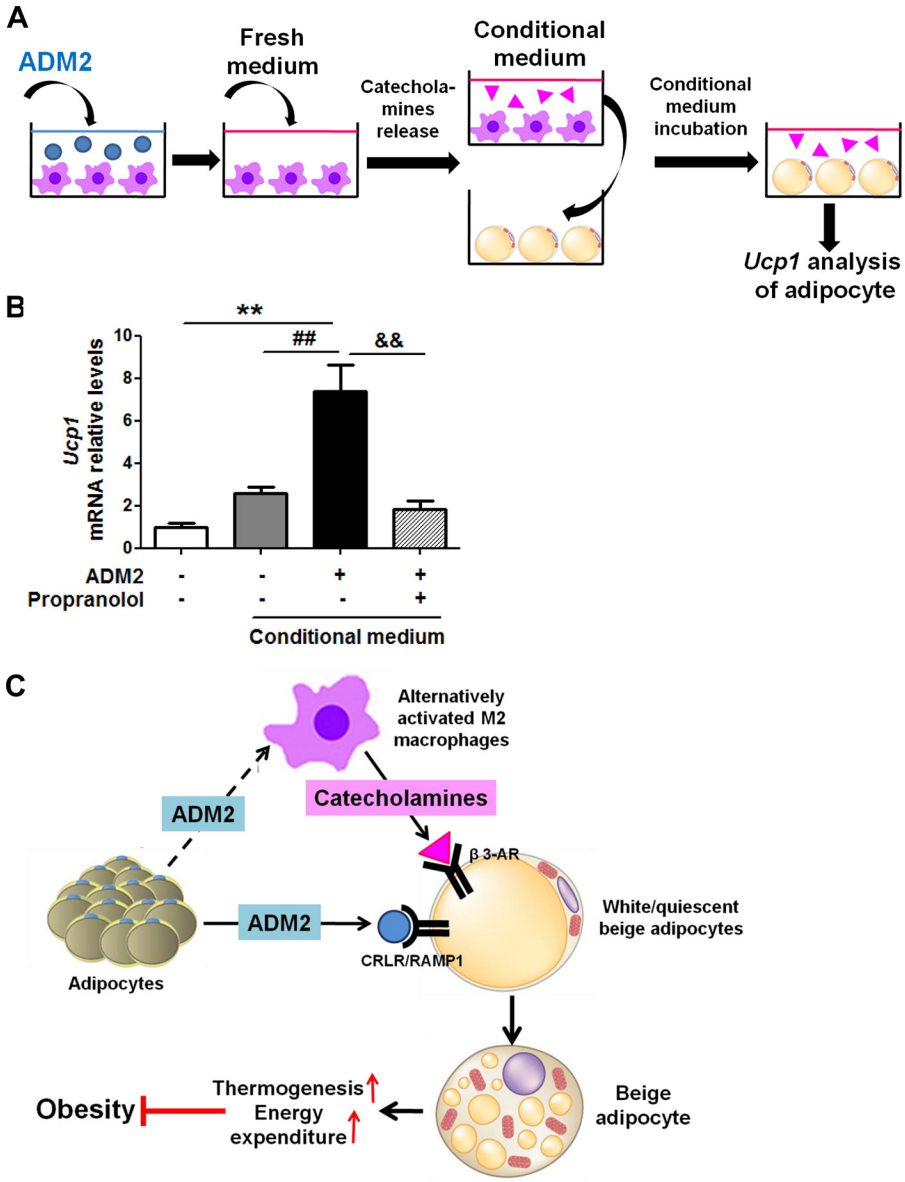

FIGURE 8. **ADM2 promotes beiging in scWAT through cross-talk between adipocytes and macrophages.** *A* and *B*, conditioned medium test. *A*, the conditional medium system for adipocytes and macrophages. After treatment with 20 nM ADM2 for 12 h, fresh medium was given to macrophages for catecholamine accumulation. Then the conditioned medium of macrophages was collected and given to adipocytes. After incubation with the medium for 8 h, adipocytes were collected for *Ucp1* mRNA analysis. *B*, relative mRNA levels of *Ucp1* in adipocytes treated with conditioned medium from ADM2-treated or control macrophages for 8 h with or without 1-h pretreatment of the β-adrenergic receptor antagonist propranolol (10 μM), and adipocytes treated with normal control medium were used as a negative control. β-Actin was used as a normalization gene. Data are represented as mean ± S.E. $n = 3$ independent experiments (3–6 samples/experiment). One-way ANOVA with Newman-Keuls test: **, $p < 0.01$ *versus* normal control medium; ##, $p < 0.01$ *versus* control conditioned medium; &&, $p < 0.01$ *versus* ADM2-treated conditioned medium. *C*, proposed model of the effects of ADM2 on WAT beiging and energy homeostasis. As an endogenous beiging activator, ADM2 interacts with the CRLR-RAMP1 receptor on adipocytes and activates beiging of white adipocytes directly. Additionally, ADM2 acts on resident macrophages in scWAT and promotes M2 polarization and catecholamine production. The catecholamine secreted locally by M2 macrophages in turn activates the β3 adrenergic receptor on adipocytes and enhances white adipocyte beiging. The induced beige adipocytes utilize UCP1 to uncouple oxidative respiration and dissipate excess energy by thermogenesis, thus improving systematic energy homeostasis and attenuating HFD-induced obesity and related metabolic disorders.

A significant increase in carbon dioxide production (VCO_2) in adipo-ADM2-tg mice was observed during daytime but not during nighttime (supplemental Fig. S2*E*). Both adipocyte metabolism and thermogenesis are under the control of circadian rhythms (42, 43). CGRP, another member of the same peptide family as ADM2, has been found to have a circadian profile of plasma concentration (44). Thus it is possible that ADM2 could function in a circadian manner to regulate beiging and metabolic thermogenesis.

To identify the effects of ADM2 in adipose tissues, an adipocyte-specific transgenic mouse model was developed using the aP2 gene promoter in this study. It has been claimed previously that the aP2 promoter is expressed in activated macrophages in addition to adipocytes (35). In adipo-ADM2-tg mice, the overexpression efficiency of the human *ADM2* gene was dramatically lower in macrophages than in adipose tissues (supplemental Fig. 1, *B* and *C*), which is consistent with other reports in which the efficiency of the

aP2 promoter in macrophages was much lower than that of adipocytes (45–47).

Because of their inducible nature and relevance to human health, thermogenic beige adipocytes have been considered a potentially new therapeutic target for energy imbalance, and the discovery of endogenous beiging activators will provide new strategies to defend against metabolic diseases. Our results revealed a direct beiging effect of ADM2 in human primary adipocytes at both the expressional and functional levels. The inverse correlation between human plasma ADM2 and BMI also suggests that ADM2 might exert an anti-obesity role in humans. These results together suggest that the mechanism of action of ADM2 revealed in rodent studies might be translatable to humans and provide a strong scientific rationale to further explore ADM2 as a potential new therapeutic target for obesity and metabolic disorders in future studies.

Experimental Procedures

Materials—Human adrenomedullin2/intermedin(1-53) (ADM2), adrenomedullin 2/intermedin(17–47) (ADM17-47), adrenomedullin(22-52) (ADM22-52), CGRP8-37, ADM2 antibody, and the RIA kit were from Phoenix Pharmaceuticals (Belmont, CA). The anti-phospho-p38 MAPK, anti-p38 MAPK, anti-phospho-PKA substrate, anti-GAPDH, and anti-β-actin antibodies were from Cell Signaling Technology (Danvers, MA). The anti-eIF5 and anti-Arginase 1 antibodies were from Santa Cruz Biotechnology (Santa Cruz, CA). The anti-UCP1, anti-TMEM26, anti-Th, anti-Dbh, and anti-Ddc antibodies were from Abcam (Cambridge, UK).

Human Subjects—Blood samples were obtained from 74 human subjects (38 men and 36 women) from the outpatient department of Beijing Chao-Yang Hospital. Basic characteristics of the human subjects are listed in supplemental Table 1. Approximately 2–3 g of adipose tissue was excised from abdominal subcutaneous fat depots of metabolically healthy human subjects undergoing abdominal surgical operations at Peking University Third Hospital. Approval from the Local Research Ethics Committee was granted for human tissue use, and the procedures used were in accordance with institutional guidelines and the Code of Ethics of the World Medical Association (Declaration of Helsinki). All patients gave their informed consent before the procedures.

Animals—The transgenic mouse line with adipocyte-specific overexpression of the *ADM2* gene (adipo-ADM2-tg mice) was generated on the C57BL/6J background with the human *ADM2* gene driven by the fatty acid-binding protein (aP2) gene promoter as described previously (29). Male adipo-ADM2-tg mice at 6–8 weeks of age and their WT littermates were housed in a temperature-controlled room (22 °C) with a 12-h light/dark cycle. Animals were fed *ad libitum* with either a normal chow diet or high-fat diet (D12492, Research Diets, New Brunswick, NJ) for 12 weeks. For the cold challenge experiment, mice were housed individually in a 4 °C chamber for 48 h. The body temperature was measured by an electric rectal thermometer. All studies followed the guidelines of the Animal Care and Use Committee of Peking University and the National Institutes of Health Guide for the Care and Use of Laboratory Animals.

Cell Culture—Primary stromal vascular cells (SVCs) were isolated from the scWAT of male Sprague-Dawley rats (160–180 g body weight) or from human scWAT biopsy samples as described previously (48, 49). The isolated SVCs were plated and cultured to confluence in DMEM/F12 (1:1) medium containing 10% FBS. For rat adipocytes, SVCs were differentiated into adipocytes in serum-free DMEM/F12 (1:1) supplemented with 5 μg/ml insulin, 33 μM biotin, and 200 pM tri-iodothyronine. After 2 days of differentiation, the differentiation mixture was removed, and cells were maintained in serum-free DMEM/F12 (1:1) for another 2–3 days before experiments. For human adipocytes, SVCs were differentiated initially in 10% FBS-DMEM/F12 (1:1) supplemented with 500 μM isobutylmethylxanthine, 5 μg/ml insulin, 0.1 μM dexamethasone, and 33 μM biotin. After 2 days of differentiation, the differentiation mixture was removed, and cells were induced for an additional 2 days with 5 μg/ml insulin and 33 μM biotin in 10% FBS-DMEM/F12 (1:1) and then maintained in 10% FBS-DMEM/F12 for further experiments. The drugs used for adipogenic differentiation were all purchased from Sigma-Aldrich (St. Louis, MO). Mouse peritoneal macrophages were isolated as described previously (25). Eight-week-old C57BL/6J male mice were injected intraperitoneally with 2 ml of 4% thioglycollate broth (BD Biosciences Clontech). Three days later, macrophages were obtained by peritoneal lavage with 8 ml of cold PBS with 10 mM EDTA and 10% FBS. Cells were plated at 1.0×10^6/ml of RPMI 1640 with 10% FBS. After incubation for 3 h at 37 °C, nonadherent cells were washed away, and adherent cells were used for treatment.

Mitochondrial Respiration Measurements—SVCs were plated into XF24 cell culture microplates and differentiated into adipocytes. Tissue samples were freshly excised from scWAT and placed into XF24 islet capture microplates as described previously (50). Mitochondrial energetics were determined by Seahorse XF flux analyzer. The OCR was measured in the basal state and in response to respiratory chain modulators injected sequentially as follows: oligomycin (1 μM for cells and 10 μM for tissues), FCCP (carbonyl cyanide *p*-trifluoromethoxyphenylhydrazone, 1 μM for cells and 8 μM for tissues), rotenone (1 μM for cells and 3 μM for tissues), and antimycin A (1 μM for cells and 12 μM for tissues). Basal, uncoupling (proton leak), or maximal respiration OCR was calculated by subtracting the OCR measured after antimycin A and rotenone addition from the OCR measured in the basal state, measured after oligomycin addition, or measured after FCCP addition, respectively. ATP production OCR was calculated as the decline in OCR in the basal state after oligomycin addition. Coupling efficiency was calculated as the ratio of the ATP production OCR to basal respiration OCR. The respiratory chain modulators were all purchased from Sigma-Aldrich. The microplates and analyzer were from Seahorse Bioscience (North Billerica, MA).

Flow Cytometry Analysis—For adipocyte staining, primary mature adipocytes isolated from scWAT were stained with anti-PE-CD137 antibody or isotype matched IgG-labeled PE. For adipose tissue macrophage staining, SVCs isolated from scWAT were stained with a mixture of anti-FITC-CD45, anti-APC-F4/80, anti-PE-CD11c, and anti-BV421-CD206 antibod-

ies. To set proper compensation and population gates, single-color positive cells were stained with each antibody alone, and cells were incubated with isotype-matched IgG labeled with FITC, APC, PE, or BV421 as negative controls. The stained cells then underwent analysis with a FACS Aria flow cytometer, and the data were analyzed using CellQuest software. The anti-BV421-CD206 antibody was from BioLegend (San Diego, CA), and other antibodies and instruments used were from BD Biosciences.

Histology of Adipose Tissues and Adipocytes—H&E staining and immunohistochemistry of scWAT paraffin sections and immunofluorescent staining of adipocytes were conducted as described previously (13, 49). Adipocytes were stained with tetramethylrhodaminemethyl ester (TMRM) for membrane potential. Lipid droplets were stained by LipidTOX, and nuclei were stained with Hoechst 33258. Immunofluorescent signals were observed with a Leica confocal microscope. All fluorescent dyes were from Invitrogen.

RNAseq Profiling—Total RNA from differentiated adipocytes was isolated using TRIzol reagent (Promega, Madison, WI). RNAseq profiling and data analysis were conducted by the Beijing Genomics Institute.

ELISA and RIA—The cellular cAMP content in differentiated adipocytes and NE released into medium by macrophages were detected using ELISA kits from Cloud-Clone Corp. (Houston, TX). The ADM2 levels in plasma or WAT homogenates were measured using an intermedin/adrenomedullin-2 RIA kit from Phoenix Pharmaceuticals.

Quantitative RT-PCR and Immunoblotting—Quantitative RT-PCR (qPCR) reactions were performed according to previous protocols (48). Relative target mRNA levels were normalized to 18S rRNA or β-actin. The primers used for qPCR analysis are listed in supplemental Table 2.

Statistical Analysis—The data are expressed as mean ± S.E. For group comparison, one-way ANOVA followed by Newman-Keuls test for post testing (multiple-group comparison) or unpaired two-tailed Student's t test (two-group comparison) was used for statistical analysis. $p < 0.05$ was considered statistically significant. For correlation analysis, linear regression was used, and the slope was considered significantly non-zero when $p < 0.05$. The value of r represents the goodness of fit.

Author Contributions—Y. L., S. Z., X. L., H. Z., Z. X., B. L., M. X., C. J., J. S., and X. W. made substantial contributions to acquisition of data or analysis and interpretation of data. Y. L., C. J., J. S., and X. W. contributed to the design of the experiments and writing of the manuscript. All the authors approved the final version of the paper. C. J. and J. S. are the guarantors of this work and, as such, had full access to all data in the study and take responsibility for the integrity of the data and the accuracy of the data analysis.

References

1. Tseng, Y. H., Cypess, A. M., and Kahn, C. R. (2010) Cellular bioenergetics as a target for obesity therapy. *Nat. Rev. Drug Discov.* **9,** 465–482
2. Nedergaard, J., Golozoubova, V., Matthias, A., Asadi, A., Jacobsson, A., and Cannon, B. (2001) UCP1: the only protein able to mediate adaptive non-shivering thermogenesis and metabolic inefficiency. *Biochim. Biophys. Acta* **1504,** 82–106
3. Bartelt, A., and Heeren, J. (2014) Adipose tissue browning and metabolic health. *Nat. Rev. Endocrinol.* **10,** 24–36
4. Cousin, B., Cinti, S., Morroni, M., Raimbault, S., Ricquier, D., Pénicaud, L., and Casteilla, L. (1992) Occurrence of brown adipocytes in rat white adipose tissue: molecular and morphological characterization. *J. Cell Sci.* **103,** 931–942
5. Wu, J., Boström, P., Sparks, L. M., Ye, L., Choi, J. H., Giang, A. H., Khandekar, M., Virtanen, K. A., Nuutila, P., Schaart, G., Huang, K., Tu, H., van Marken Lichtenbelt, W. D., Hoeks, J., Enerbäck, S., *et al.* (2012) Beige adipocytes are a distinct type of thermogenic fat cell in mouse and human. *Cell* **150,** 366–376
6. Cohen, P., Levy, J. D., Zhang, Y., Frontini, A., Kolodin, D. P., Svensson, K. J., Lo, J. C., Zeng, X., Ye, L., Khandekar, M. J., Wu, J., Gunawardana, S. C., Banks, A. S., Camporez, J. P., Jurczak, M. J., *et al.* (2014) Ablation of PRDM16 and beige adipose causes metabolic dysfunction and a subcutaneous to visceral fat switch. *Cell* **156,** 304–316
7. Harms, M., and Seale, P. (2013) Brown and beige fat: development, function and therapeutic potential. *Nat. Med.* **19,** 1252–1263
8. Brestoff, J. R., Kim, B. S., Saenz, S. A., Stine, R. R., Monticelli, L. A., Sonnenberg, G. F., Thome, J. J., Farber, D. L., Lutfy, K., Seale, P., and Artis, D. (2015) Group 2 innate lymphoid cells promote beiging of white adipose tissue and limit obesity. *Nature* **519,** 242–246
9. Sidossis, L. S., Porter, C., Saraf, M. K., Børsheim, E., Radhakrishnan, R. S., Chao, T., Ali, A., Chondronikola, M., Mlcak, R., Finnerty, C. C., Hawkins, H. K., Toliver-Kinsky, T., and Herndon, D. N. (2015) Browning of subcutaneous white adipose tissue in humans after severe adrenergic stress. *Cell Metab.* **22,** 219–227
10. Sidossis, L., and Kajimura, S. (2015) Brown and beige fat in humans: thermogenic adipocytes that control energy and glucose homeostasis. *J. Clin. Invest.* **125,** 478–486
11. Sharp, L. Z., Shinoda, K., Ohno, H., Scheel, D. W., Tomoda, E., Ruiz, L., Hu, H., Wang, L., Pavlova, Z., Gilsanz, V., and Kajimura, S. (2012) Human BAT possesses molecular signatures that resemble beige/brite cells. *PLoS ONE* **7,** e49452
12. Shinoda, K., Luijten, I. H., Hasegawa, Y., Hong, H., Sonne, S. B., Kim, M., Xue, R., Chondronikola, M., Cypess, A. M., Tseng, Y. H., Nedergaard, J., Sidossis, L. S., and Kajimura, S. (2015) Genetic and functional characterization of clonally derived adult human brown adipocytes. *Nat. Med.* **21,** 389–394
13. Qiu, Y., Nguyen, K. D., Odegaard, J. I., Cui, X., Tian, X., Locksley, R. M., Palmiter, R. D., and Chawla, A. (2014) Eosinophils and type 2 cytokine signaling in macrophages orchestrate development of functional beige fat. *Cell* **157,** 1292–1308
14. Bordicchia, M., Liu, D., Amri, E. Z., Ailhaud, G., Dessì-Fulgheri, P., Zhang, C., Takahashi, N., Sarzani, R., and Collins, S. (2012) Cardiac natriuretic peptides act via p38 MAPK to induce the brown fat thermogenic program in mouse and human adipocytes. *J. Clin. Invest.* **122,** 1022–1036
15. Fisher, F. M., Kleiner, S., Douris, N., Fox, E. C., Mepani, R. J., Verdeguer, F., Wu, J., Kharitonenkov, A., Flier, J. S., Maratos-Flier, E., and Spiegelman, B. M. (2012) FGF21 regulates PGC-1alpha and browning of white adipose tissues in adaptive thermogenesis. *Genes Dev.* **26,** 271–281
16. Gustafson, B., Hammarstedt, A., Hedjazifar, S., Hoffmann, J. M., Svensson, P. A., Grimsby, J., Rondinone, C., and Smith, U. (2015) BMP4 and BMP antagonists regulate human white and beige adipogenesis. *Diabetes* **64,** 1670–1681
17. Qian, S. W., Tang, Y., Li, X., Liu, Y., Zhang, Y. Y., Huang, H. Y., Xue, R. D., Yu, H. Y., Guo, L., Gao, H. D., Liu, Y., Sun, X., Li, Y. M., Jia, W. P., and Tang, Q. Q. (2013) BMP4-mediated brown fat-like changes in white adipose tissue alter glucose and energy homeostasis. *Proc. Natl. Acad. Sci. U.S.A.* **110,** E798–807
18. Zhang, Y., Li, R., Meng, Y., Li, S., Donelan, W., Zhao, Y., Qi, L., Zhang, M., Wang, X., Cui, T., Yang, L. J., and Tang, D. (2014) Irisin stimulates browning of white adipocytes through mitogen-activated protein kinase p38 MAP kinase and ERK MAP kinase signaling. *Diabetes* **63,** 514–525
19. Hui, X., Gu, P., Zhang, J., Nie, T., Pan, Y., Wu, D., Feng, T., Zhong, C., Wang, Y., Lam, K. S., and Xu, A. (2015) Adiponectin enhances cold-induced browning of subcutaneous adipose tissue via promoting M2 macrophage proliferation. *Cell Metab.* **22,** 279–290

20. Rao, R. R., Long, J. Z., White, J. P., Svensson, K. J., Lou, J., Lokurkar, I., Jedrychowski, M. P., Ruas, J. L., Wrann, C. D., Lo, J. C., Camera, D. M., Lachey, J., Gygi, S., Seehra, J., Hawley, J. A., and Spiegelman, B. M. (2014) Meteorin-like is a hormone that regulates immune-adipose interactions to increase beige fat thermogenesis. *Cell* **157,** 1279–1291
21. Roh, J., Chang, C. L., Bhalla, A., Klein, C., and Hsu, S. Y. (2004) Intermedin is a calcitonin/calcitonin gene-related peptide family peptide acting through the calcitonin receptor-like receptor/receptor activity-modifying protein receptor complexes. *J. Biol. Chem.* **279,** 7264–7274
22. Takei, Y., Inoue, K., Ogoshi, M., Kawahara, T., Bannai, H., and Miyano, S. (2004) Identification of novel adrenomedullin in mammals: a potent cardiovascular and renal regulator. *FEBS Lett.* **556,** 53–58
23. Hong, Y., Hay, D. L., Quirion, R., and Poyner, D. R. (2012) The pharmacology of adrenomedullin 2/intermedin. *Br J. Pharmacol.* **166,** 110–120
24. Morimoto, R., Satoh, F., Murakami, O., Totsune, K., Suzuki, T., Sasano, H., Ito, S., and Takahashi, K. (2007) Expression of adrenomedullin2/intermedin in human brain, heart, and kidney. *Peptides* **28,** 1095–1103
25. Dai, X. Y., Cai, Y., Mao, D. D., Qi, Y. F., Tang, C., Xu, Q., Zhu, Y., Xu, M. J., and Wang, X. (2012) Increased stability of phosphatase and tensin homolog by intermedin leading to scavenger receptor A inhibition of macrophages reduces atherosclerosis in apolipoprotein E-deficient mice. *J. Mol. Cell Cardiol.* **53,** 509–520
26. Dai, X. Y., Cai, Y., Sun, W., Ding, Y., Wang, W., Kong, W., Tang, C., Zhu, Y., Xu, M. J., and Wang, X. (2014) Intermedin inhibits macrophage foam-cell formation via tristetraprolin-mediated decay of CD36 mRNA. *Cardiovasc. Res.* **101,** 297–305
27. Lu, W. W., Zhao, L., Zhang, J. S., Hou, Y. L., Yu, Y. R., Jia, M. Z., Tang, C. S., and Qi, Y. F. (2015) Intermedin1–53 protects against cardiac hypertrophy by inhibiting endoplasmic reticulum stress via activating AMP-activated protein kinase. *J. Hypertens.* **33,** 1676–1687
28. Qiao, X., Wang, L., Wang, Y., Zhao, N., Zhang, R., Han, W., and Peng, Z. (2015) Intermedin is upregulated and attenuates renal fibrosis by inhibition of oxidative stress in rats with unilateral ureteral obstruction. *Nephrology* **20,** 820–831
29. Zhang, H., Zhang, S. Y., Jiang, C., Li, Y., Xu, G., Xu, M. J., and Wang, X. (2016) Intermedin/adrenomedullin 2 polypeptide promotes adipose tissue browning and reduces high-fat diet-induced obesity and insulin resistance in mice. *Int. J. Obes.* **40,** 852–860
30. Pang, Y., Li, Y., Lv, Y., Sun, L., Zhang, S., Li, Y., Wang, Y., Liu, G., Xu, M. J., Wang, X., and Jiang, C. (2016) Intermedin restores hyperhomocysteinemia-induced macrophage polarization and improves insulin resistance in mice. *J. Biol. Chem.* **291,** 12336–12345
31. Zhang, S. Y., Lv, Y., Zhang, H., Gao, S., Wang, T., Feng, J., Wang, Y., Liu, G., Xu, M. J., Wang, X., and Jiang, C. (2016) Adrenomedullin 2 improves early obesity-induced adipose insulin resistance by inhibiting the class II MHC in adipocytes. *Diabetes* **65,** 2342–2355
32. Wang, C., Hou, X. H., Zhang, M. L., Bao, Y. Q., Zou, Y. H., Zhong, W. H., Xiang, K. S., and Jia, W. P. (2010) Comparison of body mass index with body fat percentage in the evaluation of obesity in Chinese. *Biomed. Environ. Sci.* **23,** 173–179
33. Kuwasako, K., Cao, Y. N., Nagoshi, Y., Tsuruda, T., Kitamura, K., and Eto, T. (2004) Characterization of the human calcitonin gene-related peptide receptor subtypes associated with receptor activity-modifying proteins. *Mol. Pharmacol.* **65,** 207–213
34. Sugii, S., Olson, P., Sears, D. D., Saberi, M., Atkins, A. R., Barish, G. D., Hong, S. H., Castro, G. L., Yin, Y. Q., Nelson, M. C., Hsiao, G., Greaves, D. R., Downes, M., Yu, R. T., Olefsky, J. M., and Evans, R. M. (2009) PPARγ activation in adipocytes is sufficient for systemic insulin sensitization. *Proc. Natl. Acad. Sci. U.S.A.* **106,** 22504–22509
35. Makowski, L., Boord, J. B., Maeda, K., Babaev, V. R., Uysal, K. T., Morgan, M. A., Parker, R. A., Suttles, J., Fazio, S., Hotamisligil, G. S., and Linton, M. F. (2001) Lack of macrophage fatty-acid-binding protein aP2 protects mice deficient in apolipoprotein E against atherosclerosis. *Nat. Med.* **7,** 699–705
36. Cao, W., Daniel, K. W., Robidoux, J., Puigserver, P., Medvedev, A. V., Bai, X., Floering, L. M., Spiegelman, B. M., and Collins, S. (2004) p38 mitogen-activated protein kinase is the central regulator of cyclic AMP-dependent transcription of the brown fat uncoupling protein 1 gene. *Mol. Cell. Biol.* **24,** 3057–3067
37. Cao, W., Medvedev, A. V., Daniel, K. W., and Collins, S. (2001) beta-Adrenergic activation of p38 MAP kinase in adipocytes: cAMP induction of the uncoupling protein 1 (UCP1) gene requires p38 MAP kinase. *J. Biol. Chem.* **276,** 27077–27082
38. Xiang, X., Lan, H., Tang, H., Yuan, F., Xu, Y., Zhao, J., Li, Y., and Zhang, W. (2015) Tuberous sclerosis complex 1-mechanistic target of rapamycin complex 1 signaling determines brown-to-white adipocyte phenotypic switch. *Diabetes* **64,** 519–528
39. Lee, Y. H., Petkova, A. P., Mottillo, E. P., and Granneman, J. G. (2012) *In vivo* identification of bipotential adipocyte progenitors recruited by β3-adrenoceptor activation and high-fat feeding. *Cell Metab.* **15,** 480–491
40. Lee, M. W., Odegaard, J. I., Mukundan, L., Qiu, Y., Molofsky, A. B., Nussbaum, J. C., Yun, K., Locksley, R. M., and Chawla, A. (2015) Activated type 2 innate lymphoid cells regulate beige fat biogenesis. *Cell* **160,** 74–87
41. Rosenwald, M., Perdikari, A., Rülicke, T., and Wolfrum, C. (2013) Bi-directional interconversion of brite and white adipocytes. *Nat. Cell Biol.* **15,** 659–667
42. Buhr, E. D., Yoo, S. H., and Takahashi, J. S. (2010) Temperature as a universal resetting cue for mammalian circadian oscillators. *Science* **330,** 379–385
43. Shostak, A., Husse, J., and Oster, H. (2013) Circadian regulation of adipose function. *Adipocyte* **2,** 201–206
44. Trasforini, G., Margutti, A., Portaluppi, F., Menegatti, M., Ambrosio, M. R., Bagni, B., Pansini, R., and Degli Uberti, E. C. (1991) Circadian profile of plasma calcitonin gene-related peptide in healthy man. *J. Clin. Endocrinol. Metab.* **73,** 945–951
45. Jiang, C., Qu, A., Matsubara, T., Chanturiya, T., Jou, W., Gavrilova, O., Shah, Y. M., and Gonzalez, F. J. (2011) Disruption of hypoxia-inducible factor 1 in adipocytes improves insulin sensitivity and decreases adiposity in high-fat diet-fed mice. *Diabetes* **60,** 2484–2495
46. Kumar, A., Lawrence, J. C., Jr, Jung, D. Y., Ko, H. J., Keller, S. R., Kim, J. K., Magnuson, M. A., and Harris, T. E. (2010) Fat cell-specific ablation of rictor in mice impairs insulin-regulated fat cell and whole-body glucose and lipid metabolism. *Diabetes* **59,** 1397–1406
47. Wueest, S., Rapold, R. A., Schumann, D. M., Rytka, J. M., Schildknecht, A., Nov, O., Chervonsky, A. V., Rudich, A., Schoenle, E. J., Donath, M. Y., and Konrad, D. (2010) Deletion of Fas in adipocytes relieves adipose tissue inflammation and hepatic manifestations of obesity in mice. *J. Clin. Invest.* **120,** 191–202
48. Li, Y., Jiang, C., Xu, G., Wang, N., Zhu, Y., Tang, C., and Wang, X. (2008) Homocysteine upregulates resistin production from adipocytes *in vivo* and *in vitro*. *Diabetes* **57,** 817–827
49. Lyu, Y., Su, X., Deng, J., Liu, S., Zou, L., Zhao, X., Wei, S., Geng, B., and Xu, G. (2015) Defective differentiation of adipose precursor cells from lipodystrophic mice lacking perilipin 1. *PLoS ONE* **10,** e0117536
50. Dunham-Snary, K. J., Sandel, M. W., Westbrook, D. G., and Ballinger, S. W. (2014) A method for assessing mitochondrial bioenergetics in whole white adipose tissues. *Redox Biol.* **2,** 656–660